frontiers in Earth Science

REVIEW
published: 03 March 2017
doi: 10.3389/feart.2017.00018

Influence of Stress Field Changes on Eruption Initiation and Dynamics: A Review

Roberto Sulpizio * and Silvia Massaro

Dipartimento di Scienze della Terra e Geoambientali, Università degli Studi di Bari, Bari, Italy

We review here three main (first-order) mechanisms of stress variation able to influence the triggering of volcanic eruptions and the possible impact on eruption dynamics. They are short- and long-term unloading, seismic energy effects, and changes in far field stress due to geodynamic processes. We present an equilibrium equation for rupture of magma chamber and opening of a dyke up to the surface, taking into account the contribution of each mechanism within the equation. The equation considers the effect of possible superimposition of the three mechanisms with internal processes to the magmatic system, and it is also used for discussing the possible influence on eruption dynamics. The different possible contribution to the eruption triggering are discussed for each mechanism, highlighting how, in many cases, a single mechanism alone is not sufficient for driving eruptive activity if the magmatic system is not close to eruptive conditions.

Keywords: stress change, volcanic eruptions, eruptive dynamics, unloading, seismic energy, far field stress

OPEN ACCESS

Edited by:
Thorvaldur Thordarson,
University of Iceland, Iceland

Reviewed by:
Agust Gudmundsson,
University of London, UK
Sonia Calvari,
Istituto Nazionale di Geofisica e Vulcanologia, Italy

****Correspondence:***
Roberto Sulpizio
roberto.sulpizio@uniba.it

Specialty section:
This article was submitted to Volcanology, a section of the journal Frontiers in Earth Science

Received: *27 August 2016*
Accepted: *10 February 2017*
Published: *03 March 2017*

Citation:
Sulpizio R and Massaro S (2017) Influence of Stress Field Changes on Eruption Initiation and Dynamics: A Review. Front. Earth Sci. 5:18. doi: 10.3389/feart.2017.00018

INTRODUCTION

Increasing evidence supports the idea that stress changes play a fundamental role in triggering volcanic eruptions and in controlling their dynamics (Hill et al., 2002; Manga and Brodsky, 2006).

Stress changes in volcanic areas may vary in origin due to short- or long-term processes (Gudmundsson and Philipp, 2006; Andrew and Gudmundsson, 2007; Watt et al., 2008; Plateaux et al., 2014). The first includes earthquakes and landslides (Stein, 1999; Hill et al., 2002; Harris and Ripepe, 2007; Walter, 2007; Walter et al., 2007; Watt et al., 2008; De la Cruz-Reyna et al., 2010), while the second comprises unloading due to erosion and deglaciation (Davydov et al., 2005; Sigmundsson et al., 2010), tidal effects (Sohn, 2004; Cazaneve and Chen, 2010), or changes in the tectonic regime (Ventura and Vilardo, 1999; Waite and Smith, 2004; Diez et al., 2005; Miura and Wada, 2007; Lehto et al., 2010; Carbone et al., 2014). These processes superimpose to the possible local stress variations related to internal dynamics of a volcano, such as pressure increase in the magma chamber due to magma influx from depth or buoyancy induced by magma differentiation processes (Massol and Jaupart, 1999; Gudmundsson, 2006, 2016; Cañon-Tapia, 2014). Although usually claimed for explaining eruptive style transitions (i.e., from effusive to explosive, or from no-activity to eruption, Hasabe et al., 2001; Adams et al., 2006; Ida, 2007; Di Traglia et al., 2009; Schneider et al., 2012; Ripepe et al., 2013; Kereszturi et al., 2014), the magmatic processes internal to a volcano alone are sometimes not sufficient for equalling the elastic energy due to lithostatic loading (e.g., Gudmundsson, 2016; Sulpizio et al., 2016). In other cases the physical and chemical characteristics of the deposits do not support triggering mechanisms like magma mixing or bubble nucleation. For example, arrival of gas rich magma in a magmatic system or magma evolution within the chamber itself are usually claimed for explaining transitions from effusive to explosive eruptions, even in cases in which the geological evidences are lacking (i.e., the erupted material is poorly vesicular, as in the case of many basaltic eruptions; Fink et al., 1992; Wylie et al., 1999). In other cases, the arrival of fresh magma into a magma chamber is postulated as trigger magma chamber rupture and eventually fed an eruption, even in the absence of petrological evidences (i.e., mingling and mixing; e.g., Davì et al., 2011). All these considerations claim for discussion about the state of the art and perspectives about the interplay between volcanic activity and changes in the stress field. This review has not the presumption of being exhaustive of all the knowledge on stress changes and volcanic eruptions, but we will critically review the main mechanisms inducing short- and long-term stress changes at volcanoes, and their possible influence on eruption initiation and its dynamics. The review is intended to focus on the first order effects of stress change. In particular, the changing strength and strain energy due to not homogeneous lithosphere or different volcano edifice (e.g., Gudmundsson, 2012a, 2016) is not explicitly discussed, although they are implicitly contained in the equations describing the driving/resisting pressures. The review is organized in four main chapters: stress changes due to unloading, effects of seismic energy, changes in regional stress field (far field), and influence of stress change on eruption dynamics.

STRESS CHANGES DUE TO UNLOADING

The unloading processes are the most common way to change the lithostatic load. This may induce fracture initiation/propagation, which changes the lithostatic component of the stress at any point in the lithosphere and, ultimately, may result in eruption initiation. The importance of unloading processes on volcanic activity is testified by the long-term eruptive histories of many volcanoes, which reveal that changes in eruption rate and/or magma composition follows partial destruction of the edifice (Presley et al., 1997; Hildenbrand et al., 2004; Hora et al., 2007; Longprè et al., 2009; Boulesteix et al., 2012).

The unloading can be a short- or long-term process, and the different mechanisms will be reviewed following the temporal scale of action.

Long-Term Processes

Many surface load variations occurring over a long time scale (such as deglaciation at mid high latitudes) have been suggested to have a significant impact on eruptive behavior (Jellinek et al., 2004; Sinton et al., 2005; Sigmundsson et al., 2010; Geyer and Bindeman, 2011; Hooper et al., 2011). A retreating ice cap of limited dimensions and thickness (e.g., radius of only a few kilometers) will affect only the shallowest parts of a magmatic system. Conversely, a retreating ice cap with a radius of tens of kilometers or more may influence the generation of melt down to the mantle (Gudmundsson, 1986; Andrew and Gudmundsson, 2007; Sigmundsson et al., 2010).

This can be expressed in a simple way considering the expression of pressure in the elastic Earth:

$$P = p_0(\sigma_{xx} + \sigma_{yy} + \sigma_{zz}) \tag{1}$$

or, in cylindrical coordinates:

$$P = \frac{1}{3}p_0(\sigma_{xx} + \sigma_{yy} + \sigma_{zz}) \tag{2}$$

where $p_0 = rgh$, σ_{rr}, $\sigma_{\theta\theta}$, and σ_{zz} the radial, tangential and vertical stress, respectively (**Table 1**).

Considering a disc load, the vertical stress at a depth z in the Earth crust and distance R from the load center can be expressed as Davis and Selvadurai (2001) and Pinel and Jupart (2004):

$$\sigma_{zz} = p_0\left[1 - \frac{z^3}{\left(R^2 + z^2\right)^{3/2}}\right] \tag{3}$$

The other two horizontal stress components are equal to:

$$\sigma_{rr} = \sigma_{\theta\theta} = \frac{p_0}{2}\left[(1+2\nu) - \frac{2(1+\nu)z}{\sqrt{(R^2+z^2)}} + \frac{z^3}{(R^2+z^2)^{3/2}}\right] \tag{4}$$

where ν the Poisson ratio here equal to 0.5. Taking into account equations (2) to (4) the pressure under a disc load overlying an elastic space is:

$$P = \frac{2}{3}p_0(1+\nu)\left[1 - \frac{z}{\sqrt{(R^2+z^2)}}\right] \tag{5}$$

It is evident that for $R \rightarrow \infty$ both stress and pressure simplify to lithostatic. The influence of disc load is greater in the upper crust, while it decreases with depth (increasing z).

Using these equations Sigmundsson et al. (2010) calculated the influence of unloading due to melting of an ice cap (**Figure 1**). The calculations were performed for two different ice models, both with radius 50 km and constant thinning rate during 110 years. The first model has a uniform thinning rate of 50 cm year^{-1} (corresponding to surface pressure change of 4.5 kPa year^{-1}). The second model thins by 25 cm year^{-1} between 0 and 30 km, and by 62 cm year^{-1} between 30 and 50 km (**Figure 1**). It can be seen that the pressure decrease is, in average, around 4–5 kPa year^{-1} in the first 10 years, increasing up to 6–7 kPa year^{-1} after 110 years. It means an average reduction of pressure of 0.5–0.6 MPa in about one century. It is worth nothing that the main part of pressure decrease is located in the upper 10–15 km (**Figure 2**), which is also the location of shallow magma chambers and magmatic feeding/conduit systems.

The effects on a shallow magma chamber can be numerically simulated considering it as a cavity of an idealized shape (sphere or ellipsoid) within an elastic homogeneous crust and filled

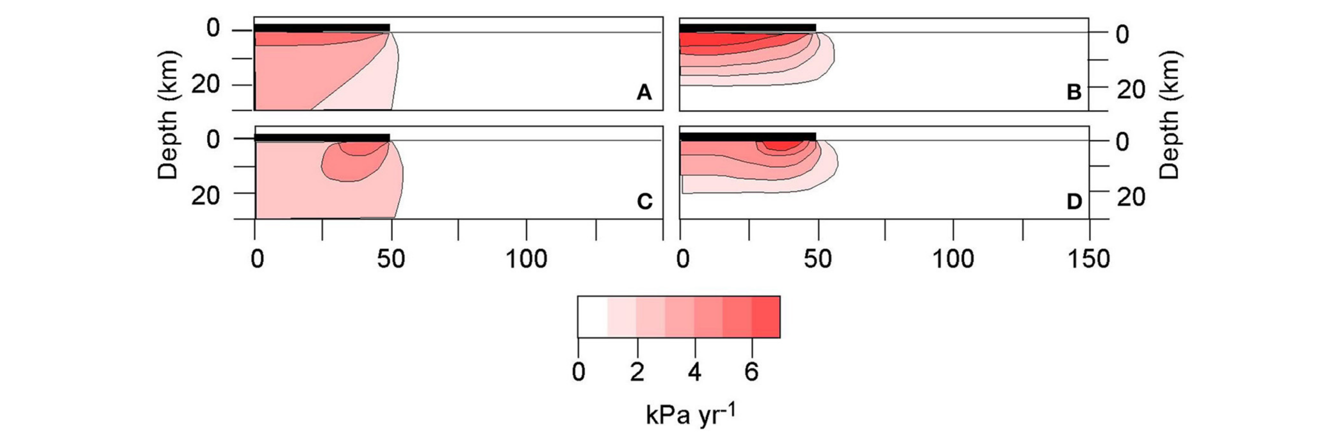

FIGURE 1 | Pressure decrease below a melting ice cap (modified after Sigmundsson et al., 2010). Results shows two different ice caps, both with radius 50 km and constant thinning rate during 110 years. **(A,B)** Uniform thinning rate of 50 cm year^{-1} (corresponding to surface pressure change of 4.5 kPa year^{-1}). **(C,D)** Thinning rate of 25 cm year^{-1} between 0 and 30 km, and of 62 cm year^{-1} between 30 and 50 km. The final volume reduction is the same in both models. **(A,C)** Average yearly stress change in the initial 10 years after thinning begins. **(B,D)** Average yearly stress changes 100–110 years after the beginning of thinning.

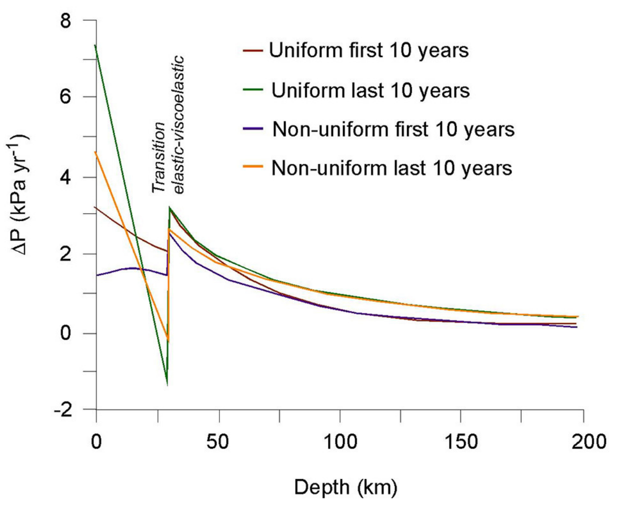

FIGURE 2 | Pressure release under an axisymmetric ice cap vs. depth, calculated for uniform and non-uniform retreating in initial 10 years and last 10 years (modified after Sigmundsson et al., 2010).

with an inviscid fluid. The magma has the same density of the surrounding crust and the reference state is lithostatic. Although strong, these assumptions can provide a first order picture of the unloading effects on a shallow reservoir (Gudmundsson, 2006).

Surface load variation induces a magma pressure change (ΔP_m) and a modification of the excess magma pressure required for dyke initiation P_e (Gudmundsson, 2012b). The failure of the chamber wall that marks the dyke initiation occurs when the minimum compressive deviatoric stress reaches the tensile strength (T_0) of the host rocks (Pinel and Jaupart, 2005; Gudmundsson, 2012b). Applying this rupture criterion in three dimensions, the ΔP required for dyke initiation can be defined (Albino et al., 2010). However, to allow dyke propagation we need a sufficient magma overpressure (P_o, also named driving pressure and net pressure, values up to several tens of MPa), which is the driving mechanism of a hydrofracture (a fluid-driven extension fracture; Gudmundsson, 2012b). Overpressure is the result of the combined effects of the initial excess pressure in the magma chamber, the (eventual) magma buoyancy, and the lithostatic load (Gudmundsson, 2006). It also acts against the normal stress applied on the potential dyke fracture before magma emplacement, and it coincides with the minimum principal compressive stress σ_3. A general form to express overpressure is (Gudmundsson, 1990, 2012b):

$$P_0 = P_e + (\rho_r - \rho_m)\, g h_1 + \sigma_d + R_f \tag{6}$$

where deviatoric stress $\sigma_d = \sigma_1 - \sigma_3$, and ρ_r is the rock density and ρ_m the magma density (**Table 1**). To allow a dyke to reach the surface and feed an eruption a minimum overpressure (ΔP_{0m}) is required, in order to maintain the dyke open (Anderson, 1936; Costa et al., 2007). Taking also into account the viscous and frictional resisting forces per unit area (R_f) the Equation (6) changes into:

$$P_0 - \Delta P_{0m} = P_e + (\rho_r - \rho_m)\, g h_1 + \sigma_d + R_f \tag{7}$$

where h_1 indicates the different height of magma column during dike propagation to the surface.

Equation (6) considers the condition for dyke initiation, while the Equation (7) highlights constrains for dyke to reach the surface and feed an eruption. Because lithospheric inhomogeneity is not here considered, Equation (7) does not contain some important constraints for dyke propagation like stress barriers, elastic mismatch, and Cook-Gordon delamination (Gudmundsson, 2011). Defining ΔF_g as the difference in gravitational force at chamber rupture and at an arbitrary time during dyke propagation [$\Delta F_g = (\rho_r$

TABLE 1 | **List of symbols used in the text and equations.**

Notation	Description	Unit
σxx, σyy, σzz	Stress component in the Cartesian coordinates	Pa
σrr, $\sigma\theta\theta$, σzz	Stress component in the Cylindrical coordinates	Pa
σ_1	Maximum stress component	Pa
σ_3	Minimum stress component	Pa
σ_d	Deviatoric stress	Pa
σ_l	Lithostatic stress	Pa
σ_e	Seismic stress	Pa
σ_{ff}	Far field stress	Pa
σ_{tec}	Homogeneous horizontal tensile stress	Pa
σ_t	Total stress field	Pa
ν	Poisson's ratio	
g	Gravitational acceleration	m/s^2
h	Height	m
h_1	Height of magma column during dike propagation	m
h_i	Height of the ice cup	m
h_r	Rock thickness	m
R	Distance from the disc load center	m
R_f	Resisting force per unit area	Pa
ρ	Crustal density	kg/m^3
ρ_m	Magma density	kg/m^3
ρ_r	Rock density	kg/m^3
ρ_i	Ice density	kg/m^3
P	Pressure	Pa
P_l	Lithostatic pressure	Pa
P_0	Driving pressure	Pa
P_e	Excess magma pressure required for dyke initiation	Pa
P_u	Unloading pressure	Pa
ΔP	Pressure variation	Pa
ΔP_m	Magma pressure change	Pa
ΔP_{om}	Minimum magma pressure change	Pa
$\Delta_P(K)$	Pressure reduction within the magma chamber induced by the removal of a surface conical load	Pa
ΔF_g	Difference in gravitational force between chamber rupture and an arbitrary time during dyke propagation	N
E	Young Modulus	Pa
K	Bulk Modulus	Pa
T_o	Tensile strength of the host rocks	Pa
V	Initial volume of the reservoir	m^3
ΔV	Volume variation of the reservoir	m^3
V_e	Erupted volume in presence of edifice collapse	m^3
V_n	Erupted volume in absence of edifice collapse	m^3
D	Effective depth accounting for the total deficit of mass with respect to before rifting	m
W	Graben width	m
z	Depth	m
z_c	Depth below the rift	m
z_{in}	Depth of the crustal reservoir	m
z_1, z_2	Depth of the dyke trajectories	m

$-\ \rho_m)g(h_1 - h)]$, it is possible to descend that for $\Delta P_{0m} < \Delta F_g + R_f$ only dyke injection is possible but not eruption.

An unloading event always reduces lithostatic load, and therefore it induces changes in σ_d because:

$$\sigma_d = \sigma_1 - \sigma_3 = \left(\rho_r h_r - \rho_i h_i\right) g - \frac{\left(\rho_r h_r - \rho_i h_i\right) g}{\nu - 1} = \left(\rho_r h_r - \rho_i h_i\right) g \left[1 - \frac{1}{\nu - 1}\right] \quad (8)$$

where ν is the Poisson's ratio, and ρ_i and h_i the density and thickness of ice cap, respectively (**Table 1**). Equation (7) can therefore be written as:

$$P_0 - \Delta P_{0m} = P_e + (\rho_r - \rho_m) gh + \left(\rho_r h_r - \rho_i h_i\right) g \left[1 - \frac{1}{\nu - 1}\right] + R_f \quad (9)$$

Magma pressure changes strongly depend on the chamber shape as well as on its depth. As a general rule, dyke propagation is favored for spherical and oblate shapes of magma chambers, whereas it is inhibited for prolated ones (Gudmundsson, 2012b).

In any case, models and simple calculations show that the reduction of stress and pressure may range between a few kPa (10 years' time span) up to less than 1 MPa, about three and one orders of magnitude less than the tensile strength of rocks. This means that, in general, the ice thinning effect on the failure of shallow magma chambers is minimal (Andrew and Gudmundsson, 2007; Sigmundsson et al., 2010), and can be decisive only if the magma batch is close to the rupture conditions.

Short-Term Processes

Numerical modeling have linked short time scale redistribution of surface loads, such as partial destruction of edifices or flank collapse events, to eruption triggering and changes in eruption style (e.g., Pinel and Jaupart, 2005; Manconi et al., 2009). Large flank collapses are common phenomena in the evolution of volcanic edifices, and sometimes these events trigger explosive eruptions (Le Friant et al., 2003; Roverato et al., 2011).

The pressure decrease induced within a magma chamber by the partial destruction of a sub-aerial volcanic edifice can be quantified using an elastic model for the two-dimensional plane strain approximation (Pinel and Jaupart, 2005). Using the same approach, Pinel and Albino (2013) calculated the effect of unloading of a conical edifice over an elastic lithosphere, obtaining similar results than the removal of the ice cap. In particular, they considered a very shallow, elliptical magma batch (top 1 km of depth) filled with fluid of the same density of the surrounding rocks and bulk modulus K. Removing a conical load of 2 km radius, 1 km height, and density 2,800 kg/m^3, induces a change in the magma chamber related to:

$$\Delta P = -K\frac{\Delta V}{V} \quad (10)$$

with V being the initial volume of the reservoir (Pinel and Albino, 2013).

In the vicinity of the reservoir the pressure variation within the crust differs from the homogeneous case (**Figure 3**), being

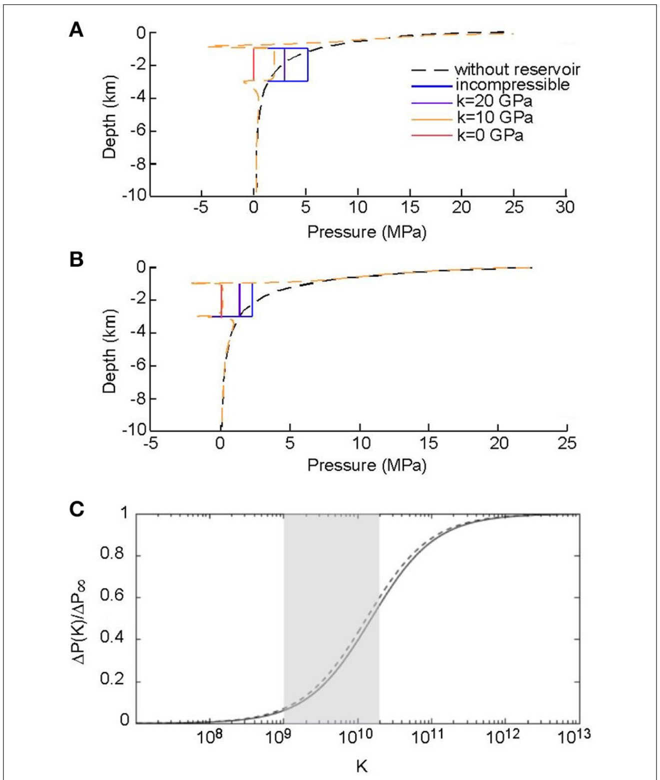

FIGURE 3 | Pressure decrease induced by unloading of a conical edifice (2 km radius, 1 km height, density of 2,800 kg/m^3) within and around a magma chamber. The reservoir is set in an elastic homogeneous space with Young modulus E = 30 GPa and Poisson ratio $\nu = 0.25$. The different lines illustrate the pressure profiles at different values of the magma bulk modulus (from incompressible to compressible magma). **(A)** Spherical chamber (radius 1 km, depth of the chamber top 1 km). **(B)** Prolate chamber (ellipsoid, half-height 1 km, half-width 0.25 km, depth of the chamber top 1 km). **(C)** Pressure reduction within the magma chamber ($\Delta P(K)$) following the removal of a surface conical load ($r = 2$ km, $h = 1$ km, density 2,800 kg/m^3) expressed as a function of the bulk modulus (K) of the magma. Crustal Young modulus and Poisson ratio are equal to 30 GPa and 0.25, respectively. The pressure change is normalized by the pressure change in a incompressible magma (ΔP_{∞}). The shaded area illustrates the characteristic values for dry magmas. The solid curve is for the spherical chamber and the dashed curve for the prolate one (modified after Pinel and Albino, 2013).

higher for spherical shape than for the prolate one. Pressure also increases at the chamber margins, and is most extreme at the chamber top. This is because the deformation of the magma chamber walls due to unloading is partially counterbalanced by pressure partition within the magma chamber.

The amount of the magma pressure reduction increases with the value of the bulk modulus. This is because for incompressible magmas (larger value of k) no reservoir volume change occurs, and only pressure lowering within the chamber compensates the reduction induced by the unloading event. The effect of compressibility is shown in **Figure 3C**.

Figure 4 shows the pressure reduction within a spherical reservoir with a top at 1 km depth, induced by the removal of the upper 20% volume of the volcano edifice (mean value based on field observations; Voight and Elsworth, 1997). The erupted volume is larger than that in the absence of edifice collapse ($V_e > V_n$; **Table 1**; **Figure 4**) when the small edifices are considered. As the edifice size increases the V_e/V_n ratio decreases. When large strato-volcanoes are partially destroyed by flank collapse this volume reduces to zero, possibly resulting in the abortion of any incipient eruption. Shallow magma batches require smaller edifice size to reach the point of aborted eruption, (**Figure 4A**), whereas deep chambers reduce any effect of edifice collapse on erupted magma volume. This is because any edifice collapse reduces the lithostatic load on the magma batch, and the magma volume required for reaching the eruptive conditions is smaller than in the case of larger edifices or deeper magma chambers (Manconi et al., 2009).

The magma reservoir shape also influences the possibility of eruption following an edifice collapse. **Figure 5** shows that the influence of the collapse is smaller for a prolate reservoir, and a larger edifice size is required than for a spherical reservoir at the same depth. Having a prolate chamber with top at depth of 1 km, eruption is only aborted when the edifice radius is greater than 6 km.

EFFECT OF SEISMIC ENERGY

Earthquakes can stress magmatic systems either through static stresses (the offset of the fault which generates a permanent deformation in the crust) or through dynamic stresses from the seismic waves (Manga and Brodsky, 2006). Both stresses increase with the seismic moment of the earthquake, but they decay in different way with distance r from the generation area. In particular, static stresses decreases as $1/r^3$, whereas dynamic stresses fall off more gradually (as $1/r^{1.66}$) and are proportional to the seismic wave amplitude (e.g., Lay and Wallace, 1995).

The stress transfer due to regional earthquakes may be of great importance in reawakening a dormant system. Previous works suggested a statistical correlation among large earthquakes and eruptions in time and space (Linde and Sacks, 1998; Hill et al., 2002; Marzocchi, 2002; Walter and Amelung, 2007; Walter et al., 2007). However, not all the large earthquakes trigger eruptions, and this is compelling evidence that the magmatic system needs to be ready to erupt under a new energetic equilibrium. This implies that the eruption triggering depends on the initial state of the magmatic system prior to the earthquake (magma composition, volatiles, chamber overpressure, strength of the host rocks, and type, size, and distance of the foci; Hill et al., 2002). In this framework, an important event is the unclamping of previous faults, which is the reduction in normal stress due to earthquake energy.

Dynamic and static deformation due to an earthquake may increase volcanic activity (Hill et al., 2002; Walter and Amelung, 2007). Seismic body and surface waves induce dynamic deformation, whereas displacement across a fault and subsequent viscoelastic relaxation of the crust account for permanent static deformation. A statistically significant response immediately after the earthquake (Linde and Sacks, 1998) has been observed for volcanoes at 750 km or more from the epicenters, suggesting they are triggered by dynamic deformation (Brodsky et al., 1998; Manga and Brodsky, 2006). The effect of static deformation

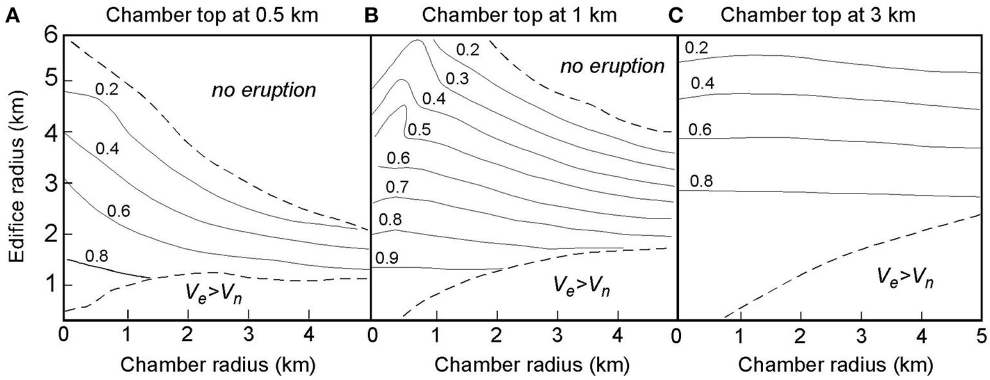

FIGURE 4 | Erupted volume of magma following the removal of the upper 20% of a conical edifice with a slope of 30°. Data presentation is function of the reservoir and edifice radius. Calculations are for a spherical magma chamber filled with incompressible magma. Crustal Poisson ratio is 0.25. Three different values for the magma chamber top depth are considered: **(A)** 0.5 km depth, **(B)** 1 km depth, **(C)** 3 km (modified after Pinel and Albino, 2013).

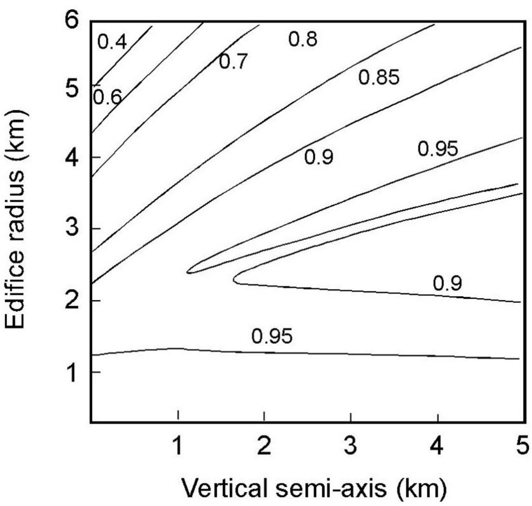

FIGURE 5 | Effects of the removal of the upper 20% volume of a conical edifice (slope of 30°) on the evolution of the erupted volume of magma. Results are presented as a contours of the reservoir vertical semi-axis and edifice radius. Calculations are for a prolate reservoir (top at 1 km depth) filled with incompressible magma. Crustal Poisson ratio = 0.25 (modified after Pinel and Albino, 2013).

in triggering eruptions remains poorly understood and it is unclear whether it is the most effective type of deformation in promoting eruptions (Marzocchi et al., 2002; Selva et al., 2004). The amplitude of static deformation decays more rapidly with distance than the seismic waves (Hill et al., 2002). Follows that to have eruption triggering from static deformation is most likely at volcanoes located in proximity to an earthquake rupture plane.

Classical examples of interaction between earthquakes and volcanic eruptions are the Kamchatka 1952 (M 9.0, followed by renewal of activity at Karpinsky and Maly Semiachik volcanoes, and at the Tao-Rusyr Caldera), Chile 1960 (M 9.5, followed by renewal of activity at Cordón-Caulle Planchón-Peteroa, Tupungatito and Calbuco volcanoes), Alaska 1964 (M 9.2, followed by renewal of activity at Trident and Redoubt volcanoes), Sumatra-Andaman 2004–2005 (M 9.3 and M 8.7, followed by renewal of activity at Talang and Barren Island volcanoes; Sepulveda et al., 2005; Walter and Amelung, 2007). All these examples are from subduction zones, which most of the time are partially locked and accumulate stress that is released during earthquakes (**Figure 6A**). Walter and Amelung (2007) related the triggering of the eruption listed above to the change in volumetric strain, which is the sum of the normal components of the strain tensor. Negative volumetric strain corresponds to volumetric contraction (compressing the rock), and positive volumetric strain corresponds to volumetric expansion (decompressing the rock). Earthquakes in subduction areas are associated with volumetric contraction in the near-trench portion of the forearc and volumetric expansion in the far-trench portion, which is where the volcanic arc is usually located (**Figure 6B**). The main observation is that all the erupted volcanoes underwent volumetric expansion induced by the earthquake. A direct mechanical effect of stress change due to volumetric expansion may be the unclamping of the fissure system. A pre-existing network of cracks may be connected, nucleate and thereby facilitate preferred paths for magma ascent. Unclamping of fracture system was claimed for the earthquake occurred on Kamchatka peninsula on January 1st, 1996 along a SW–NE trending fracture system, which triggered the twin-eruption at the volcanoes Karymsky and Akademia Nauk (Walter, 2007). The earthquake is hypothesized to have prompted dilatation of the magmatic system together with extensional normal stress at intruding N–S trending dykes, allowing magma to propagate to the surface.

Taking into account Equation (10) and adding the contribution of seismic stress, it can be written:

$$P_0 - \Delta P_{0m} = P_e + (\rho_r - \rho_m)\, gh + \left(\rho_r h_r - \rho_i h_i\right) g \left[1 - \frac{1}{\nu - 1}\right] + \sigma_e + R_f \quad (11)$$

NON-SEISMIC CHANGES IN REGIONAL STRESS FIELD

The change in tectonic stress has been claimed as trigger of large ignimbrite eruptions or for controlling the eruptive style of explosive eruptions (Korringa, 1973; Aguirre-Díaz and Labarthe-Hernandez, 2003; Miller and Wark, 2008; Costa et al., 2011).

The first order influence of far-field stress (σ_{ff}) on eruption triggering was investigated using numerical simulations, which demonstrated how the combined effect of crustal extension and magma chamber overpressure can sustain linear dyke-fed explosive eruptions with mass fluxes in excess of 10^{10} kg/s from shallow-seated (4–6 km depth) chambers affected by extensional stress regime (Costa et al., 2011). The model shows that for a far-field stress above the value able to counterbalance the lithostatic pressure at the fragmentation depth (**Figure 7**), a dyke of any length remains opened, and the Mass Eruption Rate (MER) is strongly controlled by the 3D geometry and

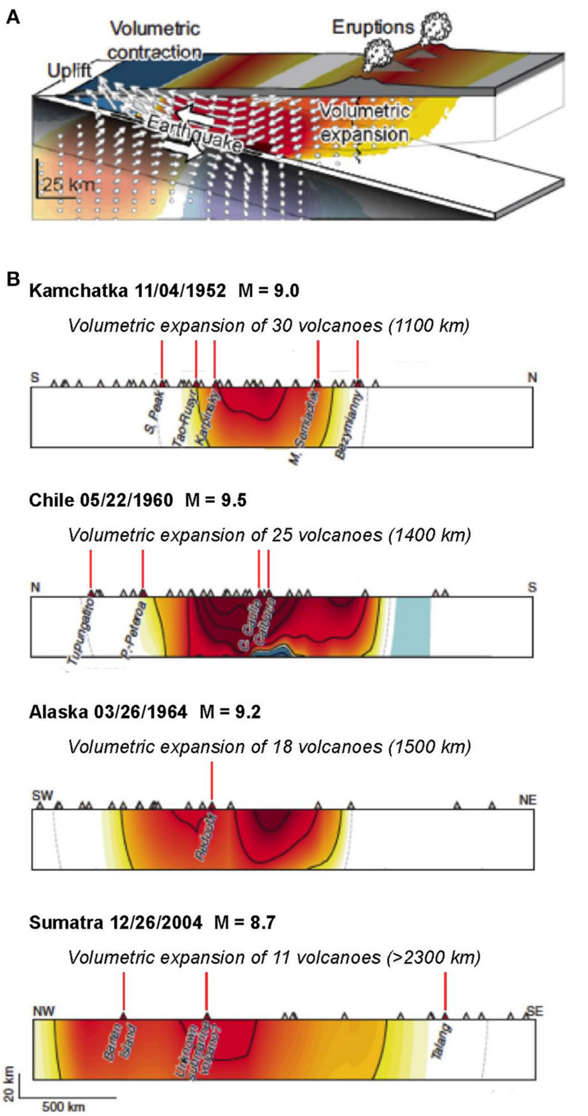

FIGURE 6 | (A) Schematic cross sections of subduction zone. Arrows indicate the displacement field, while colors rank the volumetric deformation (red colors for volumetric expansion, blue colors for volumetric contraction) associated with a megathrust earthquake. **(B)** Volumetric deformation associated with megathrust earthquakes. Triangles indicate the historically active volcanoes. Red lines highlight the volcanoes that erupted within 3 years from earthquakes. Red colors indicate positive strain (volumetric expansion), blue colors indicate negative strain (volumetric contraction). Contours represent 0 μ strain (dashed line) and 5 μ strain increments (solid black lines) (modified after Walter and Amelung, 2007).

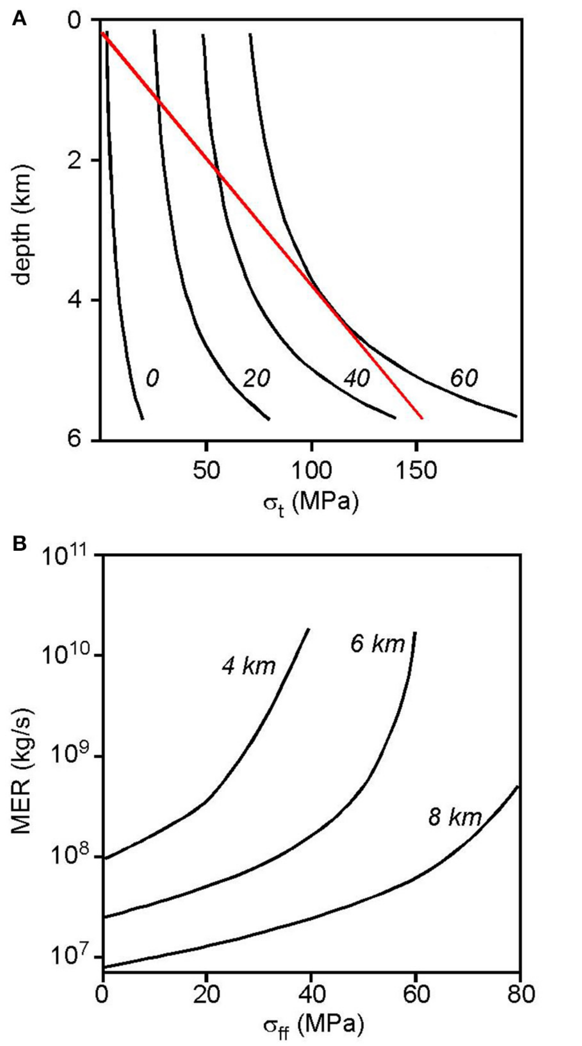

FIGURE 7 | (A) Profile of dyke tensile stress σ_t along the vertical axis obtained using the analytical solution for a pressurized magma chamber under the effect of different far-field extensional stresses. Values between 0 and 60 MPa of the far-field stresses σ_{ff} were considered for a magma chamber with circular cross-section. Red line represents the lithostatic pressure. For σ_{ff} of 40 MPa or larger the dyke remains open throughout its length and magma flow dynamics is mainly controlled by the 3D geometry and extension of the system. **(B)** Maximum Eruption Rate (MER) as a function of extensional stress σ_{ff} for a dyke thickness of 5 m for magma chambers at 4, 6, and 8 km depths and overpressures above lithostatic of 20 MPa, respectively (modified after Costa et al., 2011).

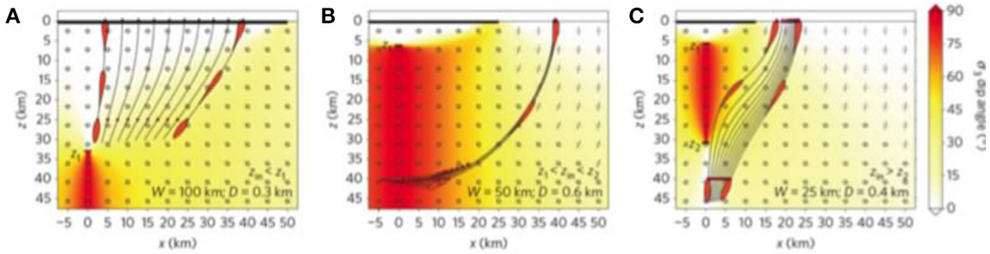

FIGURE 8 | Dyke trajectories for z_{in} above (A), within **(B)**, and below **(C)** the stress barrier zone. Red squares indicate the upper tip of the dyke at injection; red circles indicate that a dyke arrested and formed a sill; red triangles indicate the arrival location at the surface. Black and gray segments show the directions of σ_1 and σ_3, respectively (a circle indicates direction perpendicular to the page), for three nominal sets of graben width (W) and depth (D). The dip angle of σ_3 is color-shaded. Where the dip angle is subvertical (reddish color), a stress barrier to vertical ascent of dykes is acting (modified after Maccaferri et al., 2014).

extension of the system. It is worth noting that the requested value of σ_{ff} is as high as 40–60 MPa, which is not easily matched during normal geodynamic processes. As an example, a homogeneous horizontal tensile stress $\sigma_{tec} = 5$ MPa was used by Maccaferri et al. (2014) for modeling the dyke trajectories in rifting areas. In this model the dyke opens under assigned normal and shear stress given by the internal overpressure and by the shear component of the tectonic plus unloading stresses, respectively. The overpressure within the dyke is set as the difference between the magma pressure and the confining stress, which is the superposition of the lithostatic pressure, the normal component of the topographic unloading and the tectonic stress. When the unloading pressure $P_u = \rho\ gD$ (ρ is crustal density, g acceleration due to gravity, and D is the effective depth accounting for the total deficit of mass from the topographic depression and low-density sediments with respect to before rifting) dominates over the tectonic tensile stress ($D > \pi\sigma_{tec}/(2\rho g)$, 250 m for $\rho = 3{,}000$ kgm^{-3}), σ_3 becomes vertical beneath the rift in a volume centered at a depth $z_c = \rho gDW/(\pi\sigma_{tec})$, where W is the graben width (**Table 1**; **Figure 8**). The upper limit of the volume is given by $z_1 = (W/2K)(1-(1-K^2)^{1/2})$ and the lower one by $z_2 = (W/2K)(1 + (1-K^2)^{1/2})$, where $K = \pi\sigma_{tec}/(2P_0)$ (**Table 1**; Maccaferri et al., 2014).

This volume forms a stress barrier zone, which deflects the ascending dykes to the rift sides.

Sideways from the rift center, σ_3 becomes first inward dipping and then horizontal (**Figure 8**). Three scenarios for dyke propagation and for the final surface distribution of magmatism can occur, depending on where the dykes nucleate relatively to the stress barrier zone. When $z_{in} < z_1$ in-rift volcanism occurs, while off-rift volcanism occurs for $z_1 < z_{in} < z_2$ and $z_{in} > z_2$ (**Table 1**; **Figure 8**).

Incorporating the far-field tectonic stress in Equation (11) we have:

$$P_0 - \Delta P_{0m} = P_e + (\rho_r - \rho_m)\, gh + \left(\rho_r h_r - \rho_i h_i\right) g \left[1 - \frac{1}{\nu - 1}\right] + \sigma_e + \sigma_{tec} + R_f \quad (12)$$

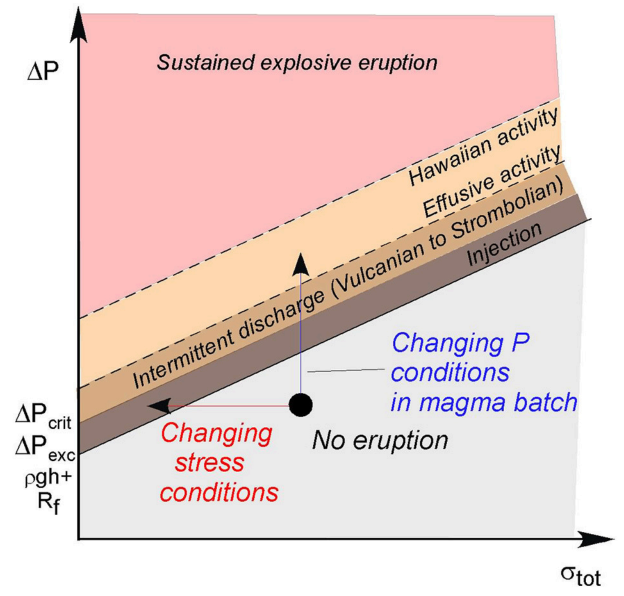

FIGURE 9 | Qualitative representation of the relationships between magmatic overpressure (ΔP) and lithostatic stress (σ_3). Eruption initiation may be triggered by an increase of ΔP at above the critical value ΔP_{crit} (the magma overpressure required to maintain a conduit open from the magma chamber to the surface) or reduction of σ_3 (after Sulpizio et al., 2016).

which is the final formulation of driving vs. resisting forces that drives the transition from no eruption to full on eruption.

INFLUENCE ON ERUPTION DYNAMICS

With the only exception of unloading due to ice cap retreat, the above discussed changes in stress field may play a role also in short term variation of eruption style. Complex transitions between effusive and explosive eruptive styles are frequently described in volcanic activity (e.g., Jaupart and Allegre, 1991; Villemant and Boudon, 1998; Adams et al., 2006; Platz et al., 2007) and the alternation of pyroclastic deposits and lavas is common in almost all stratovolcanoes. Shifts in eruptive style have been related to many complex sub-surface processes such as decompression-induced crystallization (Hammer et al., 2000; Blundy and Cashman, 2005), increase in magma viscosity due to groundmass crystallization caused by volatile loss and temperature gradients (Stevenson et al., 1996; Manga, 1998; Melnik and Sparks, 2002; Cashman and Sparks, 2013), and time-dependent release of overpressure due to the contrasting effects of magma viscosity and elastic energy released from country rocks deformation (Wylie et al., 1999).

All these processes can for sure participate to changes in eruptive style, but sharp changes in local or far-field stress may sometimes play a similar role in driving eruptive activity. This is especially true when dealing with changing eruptive style in eruptions or eruptive cycles with similar magmatic composition, which do not account for any petrologic or textural trigger of the changing eruptive behavior. For instance, the interplay between magma overpressure and stress acting on the volcanic system was claimed for explaining the eruptive style transitions of Monte dei Porri (Salina Island, Italy; Sulpizio et al., 2016), and effusive eruptions following local stress decrease due to spreading of the volcanic edifice were repeatedly observed at Mount Etna volcano (Borgia et al., 1992; Froger et al., 2001; Lundgren et al., 2004; Neri et al., 2004).

The contribution of stress lowering to the change of eruptive style can be easily explained using the Equation (12) in the ΔP vs. σ_{tot} space (**Figure 9**; Sulpizio et al., 2016). It shows how a transition from no-eruption to eruption or from a given eruptive style to another is allowed through the superimposition of internal magmatic pressure (increase of ΔP) and changing in the total stress field (σ_t), defined by the sum of all the defined partial stresses defined early.

SUMMARY AND CONCLUSIONS

Understanding the interplay between crustal stress and volcanic activity and its dynamics is essential for comprehension of a number of natural phenomena and for mitigating the related hazards and risk. Significant evidence of coupling between stress change and volcanic events emerges from investigation of tectonic earthquakes, flank collapses, and also long-term processes such as erosion and landslides. The effect of these processes superimposes on changes in magma overpressure, including the growth of gas bubbles and input of new magma in the chamber. This is because, although dyke initiation and propagation to the surface is usually governed by the depth-dependent magma parameters, the source location is also subject to the stress field conditions that vary from one point to another in the crust and that can promote or prevent brittle failures.

During last decades many authors provided precious contributions to this topic, and this review presented the state of the art of the knowledge about some of the main mechanisms inducing stress change and able to influence eruption initiation and dynamics. In particular, we reviewed three main pivotal issues correlated to stress: the unloading and its long- and short-term effects, the seismic energy, and the regional (or far-field) stress changes. Their occurrence alone was used as a preliminary guide in this study.

The contribution of each mechanism has been analyzed, and an equilibrium equation for magma chamber rupture and dyke opening to the surface has been presented. The equation was also used for interpreting the possible changes in eruptive style of single eruptions or eruptive cycles. The three mechanisms can have different impact on magmatic systems, and can influence or not the triggering of volcanic eruptions. However, it emerges clearly from this review how a single mechanism is hardly responsible for eruption initiation, but the concur of internal processes is usually necessary. It emerges how internal (magmatic processes) end external (stress field variations) processes concur in modulating eruptive activity.

AUTHOR CONTRIBUTIONS

All authors listed, have made substantial, direct and intellectual contribution to the work, and approved it for publication.

REFERENCES

Adams, N., Houghton, B. F., Fagents, S. A., and Hildreth, W. (2006). The transition from explosive to effusive eruptive regime: the example of the 1912 Novarupta eruption, Alaska. *Geol. Soc. Am. Bull.* 118, 620–634. doi: 10.1130/B25768.1

Aguirre-Díaz, G., and Labarthe-Hernández, G. (2003). Fissure ignimbrites: fissure-source origin for voluminous ignimbrites of the Sierra Madre Occidental and its relationship with Basin and Range faulting. *Geology* 31, 773–776. doi: 10.1130/G19665.1

Albino, F., Pinel, V., and Sigmundsson, F. (2010). Influence of surface load variations on eruption likelihood: application to two Icelandic subglacial volcanoes, Grimsvötn and Katla. *Geophys. J. Int.* 181, 1510–1524. doi: 10.1111/j.1365-246x.2010.04603.x

Anderson, E. M. (1936). The dynamics of formation of cone sheets, ring dykes and cauldron subsidences. *Proc. R. Soc. Edinb.* 56, 128–163. doi: 10.1017/S0370164600014954

Andrew, R. E. B., and Gudmundsson, A. (2007). Distribution, structure, and formation of Holocene lava shields in Iceland. *J. Volcan. Geotherm. Res.* 168, 137–154. doi: 10.1016/j.jvolgeores.2007.08.011

Blundy, J., and Cashman, K. (2005). Rapid decompression-driven crystallization recorded by melt inclusions from Mount St. Helens volcano. *Geology* 33, 793–796. doi: 10.1130/G21668.1

Borgia, A., Ferrari, L., and Pasquarè, G. (1992). Importance of Gravitational Spreading in the Tectonic and Volcanic Evolution of Mt. Etna. *Nature* 357:231. doi: 10.1038/357231a0

Boulesteix, T., Hildenbrand, A., Gillot, P. Y., and Soler, V. (2012). Eruptive response of oceanic islands to giant landslides: new insigths from the geomorphologic evolution of the Teide-Pico Viejo volcanic complex (Tenerife, Canary). *Geomorphology* 138, 61–73. doi: 10.1016/j.geomorph.2011.08.025

Brodsky, E. E., Sturtevant, B., and Kanamori, H. (1998). Earthquakes, volcanoes, and rectified diffusion. *J. Geophy. Res.* 103, 827–838. doi: 10.1029/98jb02130

Cañon-Tapia, E. (2014). Volcanic eruption triggers: a hierarchical classification. *Earth Sc. Rev.* 129, 100–119. doi: 10.1016/j.earscirev.2013.11.011

Carbone, D., Aloisi, M., Vinciguerra, S., and Puglisi, G. (2014). Stress, strain and mass changes at Mt. Etna during the period between the 1991–93 and 2001 flank eruptions. *Earth Sci. Rev.* 138, 454–468. doi: 10.1016/j.earscirev.2014.07.004

Cashman, K. V., and Sparks, R. S. J. (2013). How volcanoes work: a 25 year perspective. *Geol. Soc. Am. Bull.* 125, 664–690. doi: 10.1130/B30720.1

Cazaneve, A., and Chen, J. (2010). Time-variable gravity from space and present-day mass redistribution in the Earth system. *Earth Planet. Sci. Lett.* 298, 263–274. doi: 10.1016/j.epsl.2010.07.035

Costa, A., Gottsmann, J., Melnik, O., and Sparks, R. S. J. (2011). A stress-controlled mechanism for the intensity of very large magnitude explosive eruptions. *Earth Planet. Sci. Lett.* 310, 161–166. doi: 10.1016/j.epsl.2011.07.024

Costa, A., Melnik, O., and Sparks, R. S. J. (2007). Controls of conduit geometry and wallrock elasticity on lava dome eruptions. *Earth Planet. Sci. Lett.* 260, 137–151. doi: 10.1016/j.epsl.2007.05.024

Davì, M., De Rosa, R., Donato, P., and Sulpizio, R. (2011). The Lami pyroclastic succession (Lipari, Aeolian Islands): a clue for unravelling the eruptive dynamics of the Monte Pilato rhyolitic pumice cone. *J. Volcan. Geotherm. Res.* 201, 285–300. doi: 10.1016/j.jvolgeores.2010.09.010

Davis, R. O., and Selvadurai, A. P. S. (2001). *Elasticity and Geomechanics.* Cambridge, UK: Cambridge University Press 1996.

Davydov, M. N., Kedrinskii, V. K., Chernov, A. A., and Takayama, K. (2005). Generation and evolution of cavitation in magma under dynamic unloading. *J. Appl. Mechan. Technic. Physics* 46, 208–215. doi: 10.1007/s10808-005-0036-2

De la Cruz-Reyna, S., Tárraga, M., Ortiz, R., and Martínez-Bringas, A. (2010). Tectonic earthquakes triggering volcanic seismicity and eruptions. Case studies at Tungurahua and Popocatépetl volcanoes. *J. Volcan. Geotherm. Res.* 193, 37–48. doi: 10.1016/j.jvolgeores.2010.03.005

Diez, M., La Femina, P. C., Connor, C. B., Strauch, W., and Tenorio, T. V. (2005). Evidence for static stress changes triggering the 1999 eruption of Cerro Negro Volcano, Nicaragua and regional aftershock sequences. *Geoph. Res. Lett.* 32, L04309. doi: 10.1029/2004gl021788

Di Traglia, F., Cimarelli, C., de Rita, D., and Gimeno Torrente, D. (2009). Changing eruptive styles in basaltic explosive volcanism: examples from Croscat complet cone, Garrotxa Volcanic Field (NE Iberian Peninsula). *J. Volcan. Geotherm. Res.* 180, 89–109. doi: 10.1016/j.jvolgeores.2008.10.020

Fink, J., Anderson, S. W., and Manley, C. R. (1992). Textural constraints on effusive silicic volcanism: beyond the permeable foam model. *J. Geophys. Res.* 97, 9073–9083. doi: 10.1029/92JB00416

Froger, J. L., Merle, O., and Briole, P. (2001). Active spreading and regional extension at Mount Etna imaged by SAR interferometry. *Earth Planet. Sci. Lett.* 187, 245–258. doi: 10.1016/S0012-821X(01)00290-4

Geyer, A., and Bindeman, I. (2011). Glacial influence on caldera-forming eruptions. *J. Vol. Geotherm. Res.* 202, 127–142. doi: 10.1016/j.jvolgeores.2011.02.001

Gudmundsson, A. (1986). Mechanical aspects of postglacial volcanism and tectonics of the Reykjanes Peninsula, southwest Iceland. *J. Geophys. Res.* 91, 711–721. doi: 10.1029/jb091ib12p12711

Gudmundsson, A. (1990). Emplacement of dikes, sills and crustal magma chambers at divergent plate boundaries. *Tectonophysics* 176, 257–275. doi: 10.1016/0040-1951(90)90073-H

Gudmundsson, A. (2006). How local stresses control magma-chamber ruptures, dyke injections, and eruptions in composite volcanoes. *Earth Sci. Rev.* 79, 1–31. doi: 10.1016/j.earscirev.2006.06.006

Gudmundsson, A. (2011). Deflection of dykes into sills at discontinuities and magma chamber formation. *Tectonophysics* 500, 50–64. doi: 10.1016/j.tecto.2009.10.015

Gudmundsson, A. (2012a). Strengths and strain energies of volcanic edifices: implications for eruptions, collapse calderas, and landslides. *Nat. Hazards Earth Syst. Sci.* 12, 2241–2258. doi: 10.5194/nhess-12-2241-2012

Gudmundsson, A. (2012b). Magma chambers: formation, local stresses, excess pressures, and compartments. *J. Volcanol. Geotherm. Res.* 237–238, 19–41. doi: 10.1016/j.jvolgeores.2012.05.015

Gudmundsson, A. (2016). The mechanics of large volcanic eruptions. *Earth Sci. Rev.* 163, 72–93. doi: 10.1016/j.earscirev.2016.10.003

Gudmundsson, A., and Philipp, S. J. (2006). How local stress fields prevent volcanic eruptions. *J. Vol. Geotherm. Res.* 158, 257–268. doi: 10.1016/j.jvolgeores.2006.06.005

Hammer, J. E., Cashman, K. V., and Voight, B. (2000). Magmatic processes revealed by textural and compositional trends in Merapi dome lavas. *J. Volcanol. Geotherm. Res.* 100, 165–192. doi: 10.1016/S0377-0273(00)00136-0

Harris, A. J. L., and Ripepe, M. (2007). Regional earthquakes as a trigger for enhanced volcanic activity: evidence from MODIS thermal data. *Geoph. Res. Lett.* 34, L02304. doi: 10.1029/2006GL028251

Hasabe, N., Fukutani, A., Sudo, M., and Tagami, T. (2001). Transition of eruptive style in an arc-arc collision zone: K-Ar dating of Quaternary monogenetic and polygenetic volcanoes in the Higashi-Izu region, Izu peninsula, Japan. *Bull. Volcanol.* 63, 377–386. doi: 10.1007/s004450100158

Hildenbrand, A., Gillot, P., and Le Roy, I. (2004). Volcano-tectonic and geochemical evolution of an oceanic intra-plate volcano: Tahiti-Nui (french Polynesia). *Earth Planet. Sci. Lett.* 217, 349–365. doi: 10.1016/S0012-821X(03)00599-5

Hill, D. P., Pollitz, F., and Newhall, C. (2002). Earthquake-volcano interactions. *Phys. Today* 55, 41–47. doi: 10.1063/1.1535006

Hooper, A., Ofeigsson, B., Sigmundsson, F., Lund, B., Einarsson, P., Geirsson, H., et al. (2011). Increased crustal capture of magma at volcanoes with retreating ice cap. *Nat. Geosci.* 4, 783–786. doi: 10.1038/ngeo1269

Hora, J. M., Singer, B. S., and Worner, G. (2007). Volcano evolution and eruptive flux on the thick crust of the Andean Central Volcanic Zone: 40Ar/39Ar constraints from Volcan Parinacota, Chile. *GSA Bull.* 119, 343–362. doi: 10.1130/B25954.1

Ida, Y. (2007). Driving force of lateral permeable gas flow in magma and the criterion of explosive and effusive eruptions. *J. Volcanol. Geotherm. Res.* 162, 172–184. doi: 10.1016/j.jvolgeores.2007.03.005

Jaupart, C., and Allegre, C. (1991). Gas content, eruption rate and instabilities of eruption regime in silicic volcanoes. *Earth Planet. Sci. Lett.* 102, 413–429. doi: 10.1016/0012-821X(91)90032-D

Jellinek, A. M., Manga, M., and Saar, M. O. (2004). Did melting glaciers cause volcanic eruptions in eastern California? Probing the mechanics of dike formation. *J. Geophys. Res.* 109:B09206. doi: 10.1029/2004JB002978

Kereszturi, G., Nemeth, K., Cronin, S. J., Procter, J., and Augustìn-Flores, J. (2014). Influences on the variability of eruption sequences and style transitions in the Aukland Volcanic Field, New Zeland. *J. Volcanol. Geotherm. Res.* 286, 101–115. doi: 10.1016/j.jvolgeores.2014.09.002

Korringa, M. K. (1973). Linear vent area of the Soldier Meadow Tuff, an ash-flow sheet in northwestern Nevada. *Geol. Soc. Am. Bull.* 84, 3849–3866. doi: 10.1130/0016-7606(1973)84<3849:LVAOTS>2.0.CO;2

Lay, T., and Wallace, T. (1995). Modern *Global Seismology,* Vol. 58. London: Academic Press.

Le Friant, A., Boudon, G., Deplus, C., and Villemant, B. (2003). Large-scale flank collapse events during the activity of Montagne Pelè, Martinique, Lesser Antilles, *J. Geophys. Res.* 108, 2055. doi: 10.1029/2001JB001624

Lehto, H. L., Roman, D. C., and Moran, S. C. (2010). Temporal changes in stress preceding the 2004–2008 eruption of Mount St. Helens, Washington. *J. Volcanol. Geotherm. Res.* 198, 129–142. doi: 10.1016/j.jvolgeores.2010.08.015

Linde, A. T., and Sacks, I. S. (1998). Triggering of volcanic eruptions. *Nature* 395, 888–890. doi: 10.1038/27650

Longprè, M.-A., Troll, V. R., Walter, T. R., and Hansteen, T. H. (2009). Volcanic and geochemical evolution of the Teno massif, Tenerife, Canary Islands: some repercussions of giant landslides on ocean island magmatism. *Geochem. Geophys. Geosyst.* 10, Q12017. doi: 10.1029/2009GC002892

Lundgren, P., Casu, F., Manzo, M., Pepe, A., Berardino, P., Sansosti, E., et al. (2004). Gravity and magma induced spreading of Mount Etna volcano revealed by satellite radar interferometry. *J. Geophys. Res.* 31, L04602. doi: 10.1029/2003gl018736

Maccaferri, F., Rivalta, E., Keir, D., and Acocella, V. (2014). Off-rift volcanism in rift zones determined by crustal unloading. *Nat. Geosci. Lett.* 7, 297–300. doi: 10.1038/ngeo2110

Manconi, A., Longprè, M. A., Walter, T. R., Troll, V. R., and Hansteen, T. H. (2009). The effects of flank collapses on volcano plumbing systems. *Geology* 460, 1.099–1.102. doi: 10.1130/g30104a.1

Manga, M. (1998). Rheology of bubble-bearing magmas. *J. Volcanol. Geotherm. Res.* 87, 15–28. doi: 10.1016/S0377-0273(98)00091-2

Manga, M., and Brodsky, E. E. (2006). Seismic triggering of eruptions in the far field: volcanoes and geysers. *Annu. Rev. Earth Planet. Sci.* 34, 263–291. doi: 10.1146/annurev.earth.34.031405.125125

Marzocchi, W. (2002). Remote seismic influence on large explosive eruptions. *J. Geophys. Res.* 107, 2018. doi: 10.1029/2001jb000307

Marzocchi, W., Casarotti, E., and Piersanti, A. (2002). Modeling the stress variations induced by great earthquakes on the largest volcanic eruptions of the 20th Century. *J. Geophy. Res.* 107, 2320. doi: 10.1029/2001jb001391

Massol, H., and Jaupart, C. (1999). The generation of gas overpressure in volcanic eruptions. *Earth Planet. Sc. Lett.* 166, 57–70. doi: 10.1016/S0012-821X(98)00277-5

Melnik, O., and Sparks, R. S. J. (2002). "Dynamics of magma ascent and lava extrusion at Soufrière Hills Volcano, Montserrat," in *The Eruption of Soufrière Hills Volcano, Montserrat, From 1995 to 1999,* Vol. 21, eds T. H. Druitt and B. P. Kokelaar (London: Geological Society), 153–171.

Miller, C., and Wark, D. A. (2008). Supervolcanoes and their explosive supereruptions. *Elements* 4, 11–16. doi: 10.2113/GSELEMENTS.4.1.11

Miura, D., and Wada, Y. (2007). Effects of stress in the evolution of large silicic magmatic systems: an example from the Miocene felsic volcanic field at Kii Peninsula, SW Honshu, Japan. *J. Volcanol. Geotherrm Res.* 167, 300–319. doi: 10.1016/j.jvolgeores.2007.05.017

Neri, M., Acocella, V., and Behncke, B. (2004). The role of the Pernicana Fault System in the spreading of Mt. Etna (Italy) during the 2002–2003 eruption. *Bull. Volcanol.* 66, 417–430. doi: 10.1007/s00445-003-0322-x

Pinel, V., and Albino, F. (2013). Consequences of volcano sector collapse on magmatic storage zones: insights from numerical modeling. *J. Volcanol. Geotherm. Res.* 252, 29–37. doi: 10.1016/j.jvolgeores.2012.11.009

Pinel, V., and Jaupart, C. (2005). Some consequences of volcanic edifice destruction for eruption conditions. *J. Volcanol. Geotherm. Res.* 145, 68–80. doi: 10.1016/j.jvolgeores.2005.01.012

Pinel, V., and Jupart, C. (2004). Magma storage and horizontal dyke injection beneath a volcanic edifice. *Earth Planet. Sci. Lett.* 221, 245–262. doi: 10.1016/S0012-821X(04)00076-7

Plateaux, R., Béthoux, N., Bergerat, F., and Lépinay, B. M. (2014). Volcano-tectonic interactions revealed by inversion of focal mechanisms: stress field insight around and beneath the Vatnajokull ice cap in Iceland. *Front. Earth Sci.* 2:9. doi: 10.3389/feart.2014.00009

Platz, T., Cronin, S. J., Cashman, K. V., Stewart, R. B., and Smith, I. E. M. (2007). Transition from effusive to explosive phases in andesite eruptions: a case-study from the AD1655 eruption of Mt.Taranaki, New Zealand. *J. Volcanol. Geotherm. Res.* 161, 1534. doi: 10.1016/j.jvolgeores.2006.11.005

Presley, T. K., Sinton, J. M., and Pringle, M. (1997). Postshield volcanism and catastrophic mass wasting of the Waianae Volcano, Oahu, Hawaii. *Bull. Volcanol.* 58, 597–616. doi: 10.1007/s004450050165

Ripepe, M., Marchetti, E., Ulivieri, G., Harris, A., Dehn, J., Burton, M., et al. (2013). Effusive to explosive transition during the 2003 eruption of Stromboli volcano. *Geology* 33, 341–344. doi: 10.1130/G21173.1

Roverato, M., Capra, L., Sulpizio, R., and Norini, G. (2011). Stratigraphic reconstruction of two debris avalanche deposits at Colima Volcano (Mexico): insights into pre-failure conditions and climate influence. *J. Volcanol. Geotherm. Res.* 207, 33–46. doi: 10.1016/j.jvolgeores.2011.07.003

Schneider, A., Rempel, A. W., and Cashman, K. V. (2012). Conduit degassing and thermal controls on eruptive styles at Mt. St. Helens. *Earth Planet. Sci. Lett.* 357, 347–354. doi: 10.1016/j.epsl.2012.09.045

Selva, J., Marzocchi, W., Zencher, F., Casarotti, E., Piersanti, A., and Boschi, E. (2004). A forward test for interaction between remote earthquakes and volcanic eruptions: the case of Sumatra (June 2000) and Denali (November 2002) earthquakes. *Earth Planet. Sci. Lett.* 226, 383–395. doi: 10.1016/j.epsl.2004.08.006

Sepulveda, F., Lahsen, A., Bonvalot, S., Cembrano, J., Alvarado, A., and Letelier, P. (2005). Morpho-structural evolution of the Cordón Caulle geothermal region, Southern Volcanic Zone, Chile: insights from gravity and 40Ar/39Ar dating. *J. Volcanol. Geotherm. Res.* 148, 207–233. doi: 10.1016/j.jvolgeores.2005.03.020

Sigmundsson, F., Pinel, V., Lund, B., Albino, F., Pagli, C., Geirsson, H., et al. (2010). Climate effects on volcanism: Influence on magmatic systems of loading and unloading from ice mass variations with examples from Iceland. *Phil. Trans. R. Soc. Lond.* 368, 2.519–2.534. doi: 10.1098/rsta.2010.0042

Sinton, J., Gronvold, K., and Saemundsson, K. (2005). Postglacial eruptive history of the western volcanic zone, Iceland. *Geochem. Geophys. Geosyst.* 6:Q1200. doi: 10.1029/2005GC001021

Sohn, R. A. (2004). Microearthquake patterns following the 1998 eruption of Axial Volcano, Juan de Fuca Ridge: mechanical relaxation and thermal strain. *J. Geophys. Res.* 109, B01101. doi: 10.1029/2003jb002499

Stein, R. S. (1999). The role of stress transfer in earthquake occurrence. *Nature* 402, 605–609. doi: 10.1038/45144

Stevenson, R. J., Dingwell, D. B.,Webb, S. L., and Sharp, T. G. (1996). Viscosity of microlite-bearing rhyolitic obsidians: an experimental study. *Bull. Volcanol.* 58, 298–309. doi: 10.1007/s004450050141

Sulpizio, R., Lucchi, F., Forni, F., Massaro, S., and Tranne, C. (2016). Unravelling the effusive-explosive transitions and the construction of a volcanic cone from geological data: the example of Monte dei Porri eruptive cycle, Salina, Aeolian Islands (Italy). *J. Volcanol. Geotherm. Res.* 327, 1–22. doi: 10.1016/j.jvolgeores.2016.06.024

Ventura, G., and Vilardo, G. (1999). Slip tendency analysis of the Vesuvius faults: implications for the seismotectonic and volcanic hazard assessment. *Geophy. Res. Lett.* 26, 3229–3232. doi: 10.1029/1999GL005393

Villemant, B., and Boudon, G. (1998). Transition from dome-forming to plinian eruptive styles controlled by H_2O and Cl degassing. *Nature* 392, 65–69. doi: 10.1038/32144

Voight, B., and Elsworth, D. (1997). Failure of volcano slopes. *Geotechnique 47*, 535, 1–31. doi: 10.1680/geot.1997.47.1.1

Waite, G. P., and Smith, R. B. (2004). Seismotectonics and stress field of the Yellowstone volcanic plateau from earthquake first-motions and other indicators. *J. Geophys. Res.* 109, B02301. doi: 10.1029/2003JB002675

Walter, T. R. (2007). How a tectonic earthquake may wake up volcanoes: stress transfer during the 1996 earthquake–eruption sequence at the Karymsky Volcanic Group, Kamchatka. *Earth Planet. Sci. Lett.* 264, 347–359. doi: 10.1016/j.epsl.2007.09.006

Walter, T. R., and Amelung, F. (2007). Volcanic eruptions following $M \geq 9$ megathrust earthquakes: implications for the Sumatra-Andaman volcanoes. *Geology* 35, 539–542. doi: 10.1130/G23429A.1

Walter, T. R., Wang, R., Zimmer, M., Grosser, H., Luhr, B., and Ratdomopurbo, A. (2007). Volcanic activity influenced by tectonic earthquakes: static and dynamic stress triggering at Mt. Merapi. *Geophys. Res. Lett.* 34, L05304. doi: 10.1029/2006gl028710

Watt, S. F. L., Pyle, D. M., and Mather, T. A. (2008). The influence of great earthquakes on volcanic eruption rate along the Chilean subduction zone. *Earth Planet. Sci. Lett.* 277, 399–407. doi: 10.1016/j.epsl.2008.11.005

Wylie, J. J., Voight, B., and Whiteheed, J. A. (1999). Instability of magma flow from volatile dependent viscosity. *Science* 285, 1883–1885. doi: 10.1126/science.285.5435.1883

Conflict of Interest Statement: The authors declare that the research was conducted in the absence of any commercial or financial relationships that could be construed as a potential conflict of interest.